Characteristics analysis and loss optimization of the turn-on clamp circuit for IGCT based DC transformer

Yiqing Ma[1], Xueteng Tang[1], Long Zhang[1], Liang Dong[1], Fang Cai[1], Bin Cui[1], Biao Zhao[1]
[1] Tsinghua University, China

***Abstract*-- Integrated Gate Commutated Thyristors (IGCT) has a natural advantage in high voltage and large capacity power electronic equipment due to its high current processing capability. However, due to the positive feedback in the IGCT turn on process, the turn-on clamp circuit must be added to limit the switching speed which reduces system efficiency. This paper firstly introduces the working principle of opening clamp circuit. Secondly, the bus current in Modular Multilevel Converter (MMC) and Double Active Bridge (DAB) are compared, and pointed that the backflow power of DAB will significantly increase the loss of clamped circuit. In order to reduce the loss if clamped circuit and further improve the efficiency of IGCT-DAB, reducing the inductance and buffer capacitor in parallel with the IGCT were proposed, and their feasibility was analyzed. Finally, a DAB prototype of 1.5kV/3MW was constructed in MATLAB/Simulink to verify the correctness of the theory.**

***Index Terms*—IGCT, clamp circuit, DAB, ZVS**

I. Introduction

Compared with AC power grid, DC power grid has the advantages of higher system stability, convenient access to energy storage and new energy system, no reactive power, independent control of active power, and low line loss, but DC transformer are necessary for networking[1, 2]. As the core technology in DC transformer, dual-active-bridge dc–dc converter(DAB) has attracted more and more attention due to its soft-switching behavior, bidirectional power flow capability, electrical isolation and voltage conversion capabilities[3].

IGBT is widely used in power electronic transformer as a controlled semiconductor device, because IGBT has the characteristics of high voltage and large current, simple and reliable driving mode, fast switching speed. Similar to IGBT, IGCT is also a large-capacity fully controlled device. As a current-type device, IGCT has higher current-flow capacity, higher reliability, lower on-state voltage[4, 5]. Therefore, in soft switching applications, the device loss of IGCT is lower. According to[6],compared with IGBT, the system efficiency of the converter using IGCT is increased by 0.7% in the 5MW DC transformer. Due to the positive feedback of the IGCT opening process, additional turn-on clamp circuit is needed to limit *di*/*dt* at IGCT opening time to prevent overheating failure due to local chip turn-on of IGCT[7-10]. However, the clamp circuit increases system losses, reducing the advantage of IGCT solutions.

Single-phase shift(SPS) modulation is the most common DAB control scheme, and it can realize zero voltage switching(ZVS) in the full power range under voltage matching[11, 12]. Backflow power in DAB is the key to realize ZVS[13], but it will lead to increased loss of clamp circuit when the device is turned off. Therefore, compared with hard switching in MMC[14], the influence of DAB soft switching characteristics and power reflux characteristics on clamp loss needs to be analyzed. At the same time, it is significant to optimize the clamp loss to further improve the efficiency of IGCT-DAB.

The rest of the article is organized as follows. Section II introduces the working process of the clamp circuit. Section III analyzes the operating characteristics of DAB, and compare the bus current between DAB and MMC. Section IV shows the feasibility of reducing anode reactance and analyzes the impact of buffer capacitor which is paralleled in IGCT on the clamp circuit when the IGCT is turned off. Section V verifies the correctness of the theoretical analysis through simulation Finally, Section VI concludes this article.

II. The Working Process of Clamp Circuit

The working process of the clamp circuit is analyzed by bipolar MMC, due to MMC with bipolar modulation include hard turn-on and hard turn-off.

A. The Working Process when IGCT Hard Turn-On

A full-bridge submodule in IGCT-MMC is shown in Fig 1. The clamp circuit consists of anode inductor L_s, clamp capacitor C_s, clamp diode D_s and clamp resistor R_s. In MMC, the switching frequency is usually greater than the modulation frequency, the output current i_H changes a little in a switching cycle, so the constant current is used for simplified analysis. V_{ab} is the output voltage of full-bridge H_1. V_1 is the is the DC voltage of the H_1, i_{dc} is the bus current.

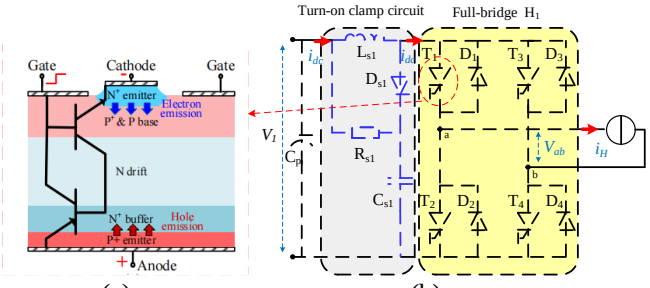

Fig. 1. IGCT-MMC (a) The chip structure of IGCT (b) The circuit diagram of IGCT-MMC

The operating waveform of the system when bipolar modulation is adopted is shown in Fig 2.

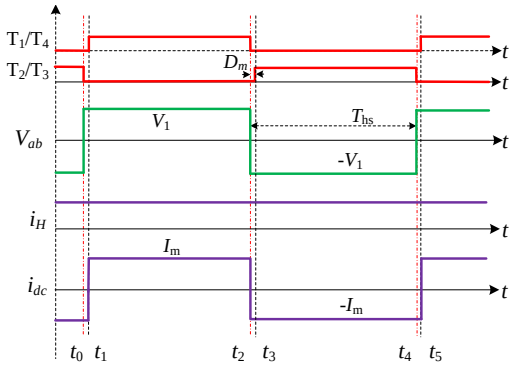

Fig. 2. The operating waveform under bipolar modulation

Where D_m is the dead time, T_{hs} is the half of the period, I_m is the maximum value of i_{dc}, the reverse recovery current I_{rr} of the diode is not drawn.

At t_0, T_2/T_3 are turned off. At this time, since the current flows through D_2/D_3, the system state does not change. i_{dc} is $-I_m$, and the positive direction is a purple arrow, as shown in Fig. 3(a). After dead time, at t_1, T_1/T_4 are turned on, the bridge arm is straight through and the output current is transferred from D_2/D_3 to T_1/T_4. Due to the reverse recovery process of D_2/D_3, i_{dc} is increased to I_m+2I_{rr}, as shown in Fig. 3(b). The effects of clamp circuit are as follows:

IGCT is a thyristor type device whose opening process is positive feedback as shown in Fig. 1(a). The current injected by the gate causes the anode carrier and cathode carrier to emit violently, which makes the device current rise rapidly without control[15]. If the current rises quickly and IGCT is not fully turned on, then the partially opened chip flows through a large current, and heat accumulation leads to device damage. In addition, diode reverse recovery cannot withstand high di/dt, so it is important to introduce anodic inductor to limit the di/dt when the bridge arm passes through.

When the reverse recovery of D_2/D_3 are completed, i_{dc} decreases, and the induced voltage generated on the anode inductor makes the clamp diode D_{s1} turn-on, and the current flowing through D_{s1} is $2I_{rr}$, as shown in Fig. 3(c). The clamp capacitor is used to absorb the energy on the anode inductor and reduce the overvoltage generated on the device.

When i_{dc} decreases to I_m, D_{s1} is turned off and the clamp capacitor discharges to the bus, as shown in Fig 3(d). The clamp resistor is used to damp the process so that the current of the anode inductor and the voltage of the clamp capacitor are restored within one operating cycle.

During the whole turn-on process, the current change diagram of anode inductor is shown in Fig. 3(e).

B. The Working Process when IGCT Turn-off

When T_1/T_4 are in on-state, T_1/T_4 conduct current and i_{dc} is I_m, as shown in Fig. 4(a). At t_2, T_1/T_4 are turned off, the output current transfers from T_1/T_4 to D_2/D_3, and i_{dc} begins to decrease, generating an induced voltage.

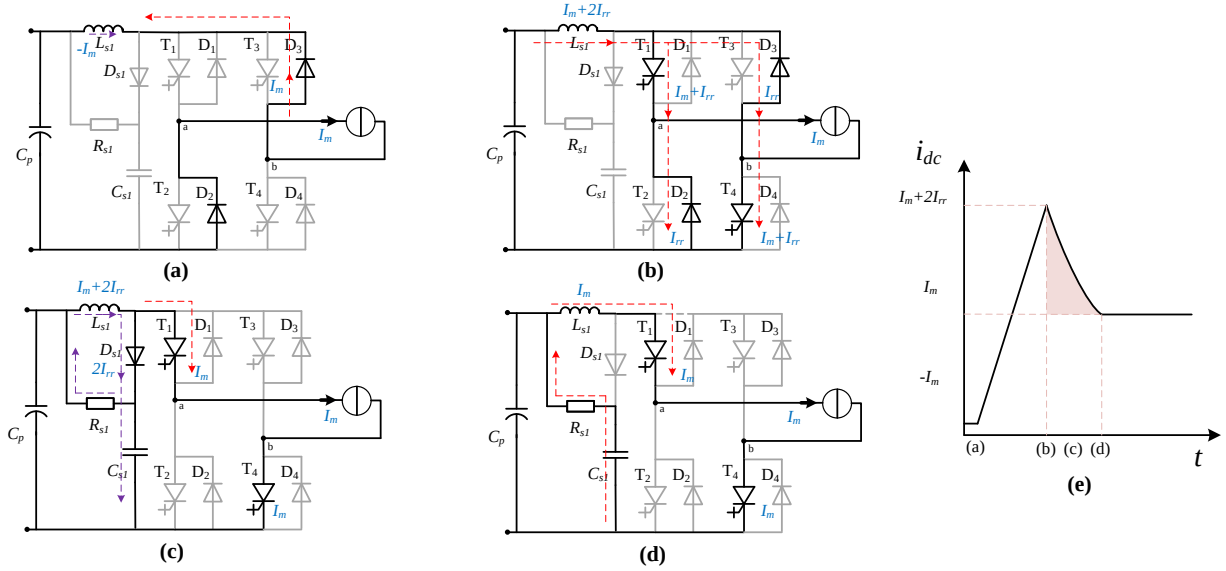

Fig.3. The working Process of T_1/T_4 hard turn-on

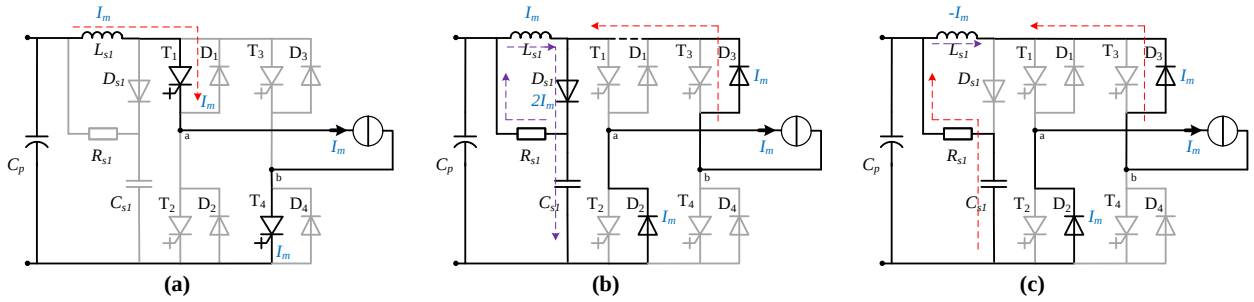

Fig.4. The working Process of T_1/T_4 hard turn-off

Therefore, the clamp diode D_{s1} is turned on, and the current flowing through D_{s1} is $2I_m$, as shown in Fig. 4(b). When i_{dc} decrease to $-I_m$, D_{s1} is turned off and the clamp capacitor discharges to the bus, as shown in Fig. 4(c).

During the whole turn-off process, the current change diagram of anode inductor is shown in Fig. 5

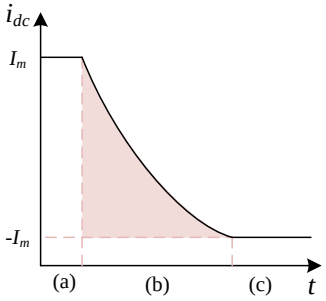

Fig.5. The current of anode inductor during IGCT turn-off

In conclusion, the clamp circuit plays a role in protecting the device when IGCT is turned on, but it also brings a certain loss. When IGCT is turned off, the clamp circuit only causes loss.

III. Comparison of Bus Current between DAB and MMC

The analysis of the clamp circuit needs to take into account the working state of the main circuit, especially the bus current because the anode inductor is in series on the bus.

A. The Bus Current Characteristics of DAB

The circuit diagram of IGCT-DAB is shown in Fig 6, which is mainly composed of full-bridge H_1/H_2, turn-on clamp circuit, auxiliary inductor and transformer.

Generally, DAB works under voltage matching V_1=nV_2, where V_1 is the is the DC voltage of the H_1, V_2 is the is the DC voltage of the H_2, n is transformer ratio. The system operating waveform under SPS control is shown in Fig 7, where D_0 is the outer phase shift ratio, D_m is the dead time, V_{ab}/V_{cd} is the output current of H_1/H_2, i_{dc} is the bus current, I_m is the maximum value of i_{dc}, i_H is the output current of H_1.,T_{hs} is the half of the period.

Before t_0, T_2/T_3 are in on-state, as shown in Fig. 8(a). At t_0, T_2/T_3 are turned off. Since i_H which is the current of auxiliary inductor and cannot be mutated, D_1/D_4 are turned on immediately, and the i_{dc} changes from I_m to $-I_m$ as shown

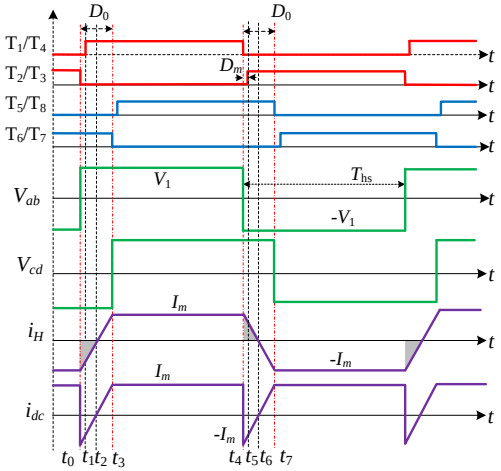

Fig. 7. The operating waveform under SPS control

in Fig. 8(b).

Due to the existence of dead time D_m, T_1/T_4 are not switched on at t_0. At t_1, T_1/T_4 are triggered to turn on for the first time with a zero-voltage but no current flowing through it. Between t_0 and t_2, a positive voltage is applied at auxiliary inductor causes i_H to rise. At t_2, i_H changes from negative to positive, and D_1/D_4 are turned off, T_1/T_4 are re-triggered and turned on with zero-voltage, as shown in Fig. 8(c). At this time, the opening di/dt of IGCT is determined by the auxiliary inductor and the system voltage. The value of the auxiliary inductance is determined by (1), which is usually much higher than the anode inductor.

$$L = \frac{nV_1V_2D_0\left(1-D_0\right)}{2fP_a} \tag{1}$$

Where, P_a rated power, f is the switching frequency.

Between t_0- t_2, DAB works in the state of backflow power, backflow current is the key to IGCT with zero voltage switching, but it also causes the bus current to change from I_m to $-I_m$.

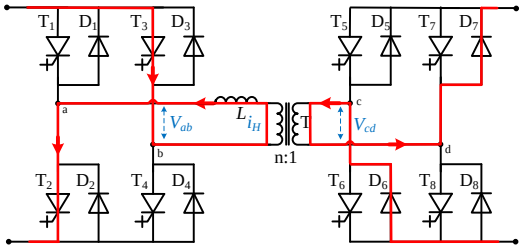

(a)

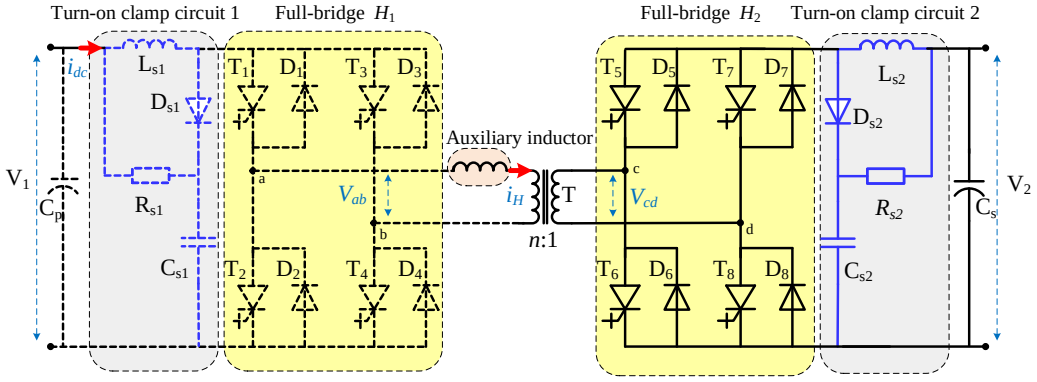

Fig. 6. The circuit diagram of IGCT-DAB

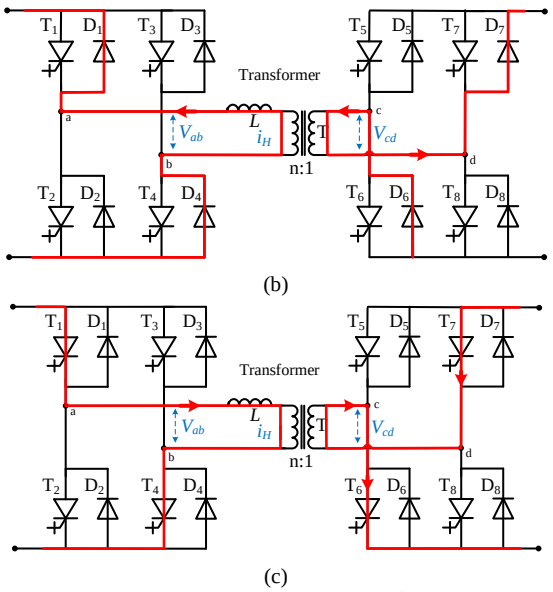

Fig. 8. The commutation process of DAB

(a) Before t_0 (b) t_0- t_2 (c) t_2- t_3

At t_3, T_6/T_7 are turned off. Similar to T_2/T_3, the change of the bus current of H_2 from I_m to $-I_m$. The turn-on process of T_5/T_8 are similar to T_1/T_4, the opening speed is limited by the auxiliary inductance.

Due to symmetry, all IGCTs in DAB are in the state of zero voltage and small di/dt when turned on, but turn-off at a large current.

B. The Bus Current Characteristics of MMC

The bus current characteristics of MMC with bipolar modulation is analyzed in the second section. In fact, the unipolar modulation is more common.

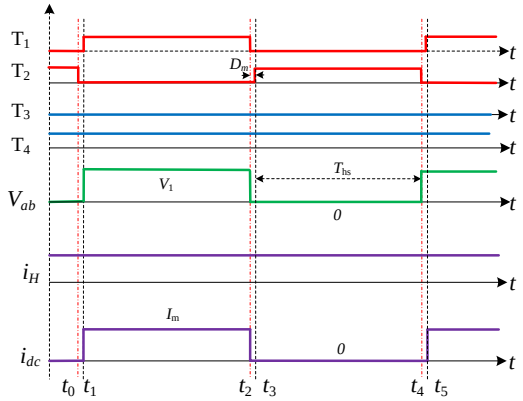

Fig. 9. The operating waveform of unipolar modulation

The system waveform with unipolar modulation is shown in Fig 9. The bridge voltage outputs V_1 and 0. At t_0, T_2 is turned off. At this time, since the current flows through D_2, the system state does not change. After the dead time ended, at t_1, T_1 is turned on, D_2 has reverse recovery process, i_{dc} changes from $-I_m$ to I_m+I_{rr}, When D_2 is turned off, i_{dc} changes to I_m. At t_4, T_1 is turned off, i_{dc} is from I_m to 0.

In conclusion, i_H of DAB changes in one switching cycle while that of MMC remains unchanged, resulting in two hard turn-off for DAB, when one hard turn-on and one hard turn-off for MMC. The switching state and bus current of DAB and MMC are summarized in Table 1.

TABLE I
COMPARISON OF DAB AND MMC

Type	Switch state	i_H	Bus current
DAB	T_2/T_3 turn off	<0	I_m/$-I_m$
	T_1/T_4 turn on		—
	T_1/T_4 turn off	>0	I_m/$-I_m$
	T_2/T_3 turn on		—
MMC (Bipolar Modulation)	T_2/T_3 turn off	>0	—
	T_1/T_4 turn on		$-I_m/(I_m+2I_{rr})/I_m$
	T_1/T_4 turn off		I_m/$-I_m$
	T_2/T_3 turn on		—
MMC (Unipolar Modulation)	T_2 turn off		—
	T_1 turn on		$0/(I_m+I_{rr})/I_m$
	T_1 turn off		$I_m/0$
	T_2 turn on		—

In the above process, when the IGCT is hard turned on, the clamp circuit limits the di/dt of the IGCT but produces loss. When IGCT is hard turned off, the clamp circuit has no beneficial effect and only produces loss.

Since the loss of the clamp circuit is proportional to the square of the attenuation of the clamp current, so the loss of the clamp circuit when IGCT is hard turned on is as follows:

$$P_{on\_loss} = k(2I_{rr})^2 \tag{2}$$

Where k is the loss factor. The loss of clamp circuit when IGCT is hard turned off is (3) in DAB and MMC with bipolar modulation, and (4) in MMC with unipolar modulation.

$$P_{off1\_loss} = k(2I_m)^2 \tag{3}$$

$$P_{off2\_loss} = kI_m^2 \tag{4}$$

When I_{rr}=I_m, combined with the Table I, the loss of the clamp circuit of DAB is approximately four times that of MMC with unipolar Modulation. When I_{rr} decreases, the ratio further increases. In order to further improve the efficiency of IGCT-DAB, it is necessary to optimize the clamp circuit loss.

IV. OPTIMIZATION OF CLAMP LOSS

This section proposes and analyzes two methods to reduce the loss of clamp circuit in DAB.

A. Reduce the value of anode inductor

In the heavy-load of DAB, all IGCTs are ZVS, and the opening speed is determined by the bus voltage and auxiliary inductor. But in the light-load or zero-load, IGCT will lose ZVS due to the effect of dead time and device parasitic capacitance. Luckily, there are many schemes such as auxiliary resonant commutated pole[16] and additional excitation inductor[17], which can realize ZVS of IGCT under the full power range. Therefore, the clamp circuit has no effect during normal operation. However, in order to ensure the safety of IGCT when the system is started, it is still necessary to select a suitable anode inductor.

The value of anode inductance is determined by (5) :

$$L = \frac{mV}{di/dt} \tag{5}$$

Where, m is the redundancy factor and V is the voltage of IGCT. All IGCTs are in the block state before the system starts, and T_1 and T_2 jointly bear the bus voltage. This means that when designing the anode reactor in DAB,

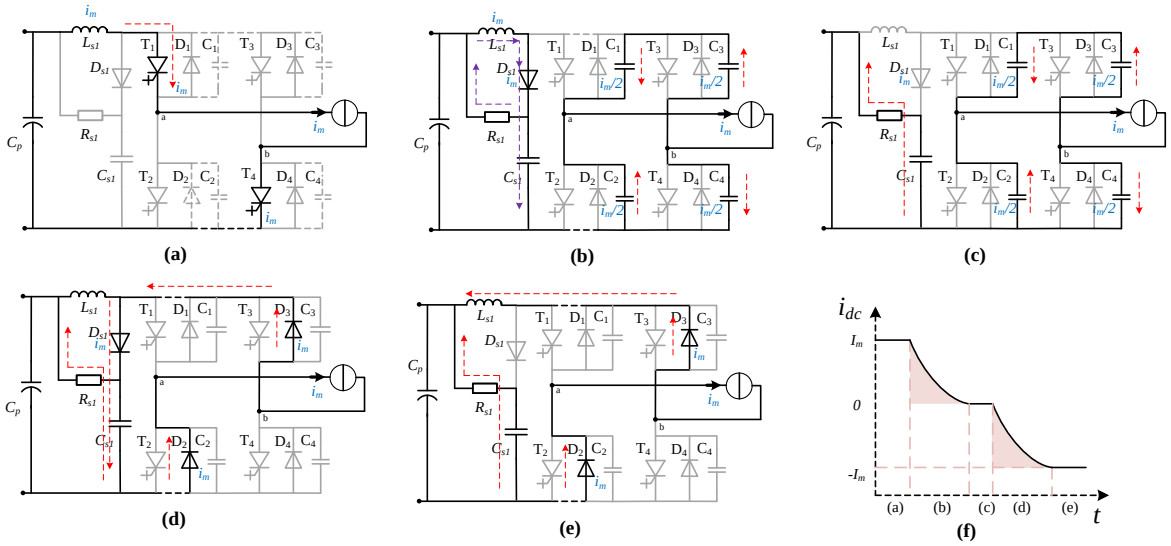

Fig.10. The working Process of T_1/T_4 turn-off with buffer capacitor

only the half bus voltage of IGCT at the start time should be considered, and there is no IGCT hard turn on under the bus voltage. According to (5), compared with MMC, the value of anode inductor in DAB can be reduced by half without affecting the reliability of the system when *di*/*dt* of IGCT is kept unchanged. The clamp circuit loss is reduced by 50% in DAB after optimization.

B. Parallel buffer Capacitor

Parallel buffer capacitance is a common way to reduce the turn-off loss of devices, but its effect on clamp circuits in DAB has not been studied.

After parallel buffer capacitor, the switching process of DAB is shown in Fig 10, and the operating waveform is shown in Fig 7. Before t_4, T_1/T_4 are in on state, T_1/T_4 conduct current and i_{ds} is I_m, as shown in Fig. 10(a). When T_1/T_4 are turned off, the load current is transferred from T_1/T_4 to the buffer capacitor C_1-C_4, and the current of the anode inductor begins to attenuate, generating an induced voltage that makes the clamp diode D_{s1} turn on, and the current flowing through D_{s1} is I_m, as shown in Fig. 10(b). When the current of the anode inductor attenuates to 0, D_{s1} is turned off and the clamp capacitor discharges to the bus, as shown in Fig. 10(c). Note that the attenuation time of the anode inductor current should be controlled to be less than the charging time of the buffer capacitor.

When the voltage of buffer capacitor C_2/C_3 drops to zero, the D_2/D_3 will be turned on. Similarly, the current of the anode inductor starts to reverse increase, generating the induced voltage to turn on the clamp diode D_{s1} again, and the current flowing through D_{s1} is I_m, as shown in Fig. 10(d). When the current of the anode inductor becomes $-I_m$, D_{s1} is turned off and the clamp capacitor C_{s1} discharges to the bus, as shown in Fig. 10(e).

During the whole process, the current of the anode inductor is shown in Figure 10(f) Therefore, the parallel buffer capacitor in DAB divides the operation of the clamp circuit when IGCT is turned off in two processes, and the attenuation process of the anode inductor current is respectively from I_m to 0 and 0 to $-I_m$. Compared to the direct attenuation of the current from I_m to $-I_m$. the clamp loss is reduced by about 50% because the energy of the inductor depends on the square of the current.

V. Simulation Verification

A 1500V/3MW IGCT-DAB model is built in MATLAB/Simulink. the system topology is shown in Fig.6, but the buffer capacitance is added and the specific parameters are shown in Table II.

TABLE II
PARAMETERS OF IGCT-DAB

Parameters	Value
DC voltage V_1/V_2 (V)	1500
Anode inductance L_{s1}(μH)	0.375
Clamp capacitance C_{s1}(μF)	30
Clamping resistor R_{s1}(Ω)	2
Buffer capacitance C_1(μF)	5.55
Auxiliary inductance (μH)	130.5
Bus capacitance C_p(mF)	25
Switching frequency (Hz)	600
the ratio of isolated transformer	1:1

Fig. 11 respectively show the simulation waveforms of anode inductor current, clamp capacitor voltage and clamp resistor current of DAB with and without buffer capacitor and the turn-off current is 1200A.

It can be seen that with the buffer capacitor, the clamp current attenuation is divided into two processes, and the peak voltage of the clamp capacitor is reduced from 2000V to 1700V. In addition, the loss of clamp circuit can be calculated based on the current flowing through the clamp resistor. Simulation shows that the loss of clamp resistance with buffer capacitor is about 0.49J and 1.08J without buffer capacitor. The loss is reduced by 54.6% through parallel buffer capacitor.

With the buffer capacitor, the clamp current will superimpose a high frequency shock, which is inevitable, because the anode inductor and buffer capacitor, bus capacitor form a loop which has no resistor. The line resistor in the actual system will make the shock attenuation quickly, and the shock decreases with the reduction of buffer capacitance, without affecting the normal operation of the system.

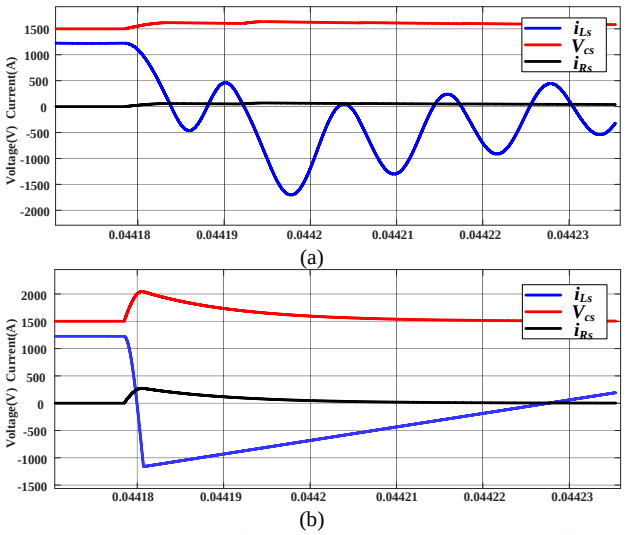

Fig. 11: The simulation of clamp circuit when T_1/T_4 is turned off (a) with buffer capacitor (b) without buffer capacitor

VI. Conclusion

DAB is known as the core circuit of the new generation circuit due to its characteristics of large power density and high efficiency. IGCT-DAB topology can give full play to the characteristics of low on-state loss of IGCT. By comparing the operating characteristics of MMC and DAB, this paper points out that the loss of clamping circuit in DAB is about four times that of MMC with the same voltage and current level. By analyzing the working condition of the clamp circuit, the anode inductor of DAB can be reduced to half of the MMC without affecting the reliability of the system operation. In addition, with full range ZVS operation, buffer capacitors can directly be paralleled without the need to withstand surge current in DAB. The loss of clamp circuit and the loss of IGCT turn-off can be further reduced after the parallel buffer capacitor, which makes the system more efficient. Finally, it is proved that the loss of the clamp circuit can be reduced by about 50% after the parallel buffer capacitor in Simulink.

References

[1] M. Starke, L. M. Tolbert, and B. Ozpineci, "AC vs. DC distribution: A loss comparison," in 2008 IEEE/PES Transmission and Distribution Conference and Exposition, 21-24 April 2008, pp. 1-7.

[2] S. Inoue, and H. Akagi, "A Bidirectional DC–DC Converter for an Energy Storage System With Galvanic Isolation," IEEE Transactions on Power Electronics, vol. 22, no. 6, pp. 2299-2306, Nov 2007.

[3] B. Zhao, Q. Song, W. Liu, and Y. Sun, "Overview of Dual-Active-Bridge Isolated Bidirectional DC–DC Converter for High-Frequency-Link Power-Conversion System," IEEE Transactions on Power Electronics, vol. 29, no. 8, pp. 4091-4106, Aug 2014.

[4] P. Ladoux, N. Serbia, and E. I. Carroll, "On the Potential of IGCTs in HVDC," IEEE Journal of Emerging and Selected Topics in Power Electronics, vol. 3, no. 3, pp. 780-793, 2015.

[5] B. Zhao, R. Zeng, Z. Yu, Q. Song, Y. Huang, Z. Chen, and T. Wei, "A More Prospective Look at IGCT: Uncovering a Promising Choice for dc Grids," IEEE Industrial Electronics Magazine, vol. 12, no. 3, pp. 6-18, Sep 2018.

[6] N. Soltau, H. Stagge, R. W. D. Doncker, and O. Apeldoorn, "Development and demonstration of a medium-voltage high-power DC-DC converter for DC distribution systems," in 2014 IEEE 5th International Symposium on Power Electronics for Distributed Generation Systems (PEDG), 24-27 June 2014, pp. 1-8.

[7] A. Boutry, C. Buttay, B. Asllani, B. Lefebvre, E. Vagnon, and D. Dong, "Experimental study of the reduction and removal of turn-on snubber for IGCT based MMC submodule using fast silicon diodes," in 2022 24th European Conference on Power Electronics and Applications (EPE'22 ECCE Europe), 5-9 Sept. 2022, pp. P.1-P.11.

[8] I. Etxeberria-Otadui, J. San-Sebastian, U. Viscarret, I. Perez-de-Arenaza, A. Lopez-de-Heredia, and J. M. Azurmendi, "Analysis of IGCT current clamp design for single phase H-bridge converters," in 2008 IEEE Power Electronics Specialists Conference, 15-19 June 2008, pp. 4343-4348.

[9] W. Yue, L. Ning, Z. Changsong, C. Wulong, L. Wanjun, and W. Zhao'an, "A clamping circuit parameter design method for IGCT used in high power applications," in 2014 IEEE Applied Power Electronics Conference and Exposition - APEC 2014, 16-20 March 2014, pp. 3406-3410.

[10] T. Wei, Q. Song, J. Li, B. Zhao, Z. Chen, and R. Zeng, "Experimental evaluation of IGCT converters with reduced di/dt limiting inductance," in 2018 IEEE Applied Power Electronics Conference and Exposition (APEC), 4-8 March 2018, pp. 1710-1716.

[11] R. W. D. Doncker, D. M. Divan, and M. H. Kheraluwala, "A three-phase soft-switched high power density DC/DC converter for high power applications," in Conference Record of the 1988 IEEE Industry Applications Society Annual Meeting, 2-7 Oct. 1988, pp. 796-805 vol.1.

[12] R. W. A. A. D. Doncker, D. M. Divan, and M. H. Kheraluwala, "A three-phase soft-switched high-power-density DC/DC converter for high-power applications," IEEE Transactions on Industry Applications, vol. 27, no. 1, pp. 63-73, 1991.

[13] F. Xu, J. Liu, and Z. Dong, "Minimum Backflow Power and ZVS Design for Dual-Active-Bridge DC–DC Converters," IEEE Transactions on Industrial Electronics, vol. 70, no. 1, pp. 474-484, Jan 2023.

[14] X. Sun, R. Bai, F. Zhuo, B. Zhao, Y. Lou, Q. Liu, and X. Wang, "Measurement and analysis of clamp circuit loss of IGCT-MMC sub-module," in 2021 Annual Meeting of CSEE Study Committee of HVDC and Power Electronics (HVDC 2021), 28-30 Dec. 2021, vol. 2021, pp. 401-405.

[15] R. Bai, B. Zhao, T. Zhou, X. Tang, J. Li, B. Cui, Z. Yu, and R. Zeng, "PWM-Current Source Converter Based on IGCT-in-Series for DC Buck and Constant-Current Application: Topology, Design, and Experiment," IEEE Transactions on Industrial Electronics, vol. 70, no. 5, pp. 4865-4874, May. 2023.

[16] N. Soltau, J. Lange, M. Stieneker, H. Stagge, and R. W. D. Doncker, "Ensuring soft-switching operation of a three-phase dual-active bridge DC-DC converter applying an auxiliary resonant-commutated pole," in 2014 16th European Conference on Power Electronics and Applications, 26-28 Aug. 2014, pp. 1-10.

[17] G. Xu, L. Li, X. Chen, W. Xiong, X. Liang, and M. Su, "Decoupled EPS Control Utilizing Magnetizing Current to Achieve Full Load Range ZVS for Dual Active Bridge Converters," IEEE Transactions on Industrial Electronics, vol. 69, no. 5, pp. 4801-4813, May 2022.